

SURFACE HEAT FLUX ANALYSIS IN URBAN AREAS USING ASTER AND MODIS DATA

Yasushi Yamaguchi, Soushi Kato, and Ken Okamoto

Department of Earth and Planetary Sciences, Graduate School of Environmental Studies

Nagoya University, Furo-cho, Chikusa-ku, Nagoya, 464-8601, Japan

Email: yasushi@nagoya-u.jp

ABSTRACT

The urban heat island occurs as a result of increase of the sensible heat flux from the land surface to the atmosphere. We have successfully developed a new method by which to evaluate separately the contributions of anthropogenically discharged heat and natural heat radiation to heat flux based on a heat balance model using satellite remote sensing and ground meteorological data. This method was applied for the ASTER and ETM+ data of Nagoya, Japan. The increased sensible heat flux due to anthropogenic activities in the central part of the city was approximately twice that in the surrounding residential areas during summer. We also used MODIS data to estimate temporal variations of surface heat fluxes in urban areas. In daytime, the sensible heat flux was high in urban areas, while it was nearly zero in all areas in nighttime. This study showed that combination of ASTER/ETM+ and MODIS data is a powerful tool to analyze the spatial and temporal variations of surface heat fluxes in urban areas.

1 INTRODUCTION

The urban heat island effect occurs as a result of increased sensible heat flux from the land surface to the atmosphere. Sensible heat flux consists of two components, exhausted anthropogenic heat and heat radiation due to solar input, of which the later may be enhanced by changes in the usage of artificial land surface. We analyzed surface heat fluxes in an urban area by using satellite remote sensing data and ground meteorological data.

The Advanced Spaceborne Thermal Emission and Reflection Radiometer (ASTER) is a high spatial resolution multi-spectral imaging radiometer onboard the NASA's Terra spacecraft launched in December, 1999 (Yamaguchi *et al.*, 1998, 2001). ASTER has 14 spectral bands in the visible to thermal infrared regions with 15 to 90 m spatial resolution and 60 km imaging swath. ASTER data are available from either the ASTER Ground Data System (GDS) of Earth Remote Sensing Data Analysis Center (ERSDAC) in Japan or EROS Data Center (EDC) of the U.S. Geological Survey in U.S.A. For more details and updates, please visit the following web sites; <http://www.ersdac.or.jp/eng/index.E.html> or <http://asterweb.jpl.nasa.gov/>. ETM+ is a multi-spectral imaging radiometer on Landsat satellite with 7 spectral bands, 15 to 60 m spatial resolution, and 180 km imaging swath.

2 METHOD

2.1 ASTER data analysis

For natural land surface, absorbed net radiation should balance outgoing fluxes of ground heat, sensible heat and latent heat (Schmugge *et al.*, 1998):

$$R_n = G_n + LE_n + H_n \quad (1)$$

where R_n is net radiation, G_n is ground heat flux, LE_n is latent heat flux, and H_n is sensible heat flux. Net radiation is the sum of incoming solar and long-wave radiations emitted from the atmosphere to land surface and from the land surface to the atmosphere. During the day, ground heat is conducted into the ground, because the underground temperature is generally lower than the surface temperature. Latent heat is produced by transpiration of vegetation and evaporation of land surface water. The remaining energy increases the surface temperature and is transferred from land surface to the atmosphere as sensible heat (Figure 1).

However, in urban areas, in addition to the net radiation, the anthropogenic heat discharge also causes heat fluxes. We introduce H_a as sensible heat flux due to anthropogenic activities, while H_n is sensible heat flux originated from the net radiation. Satellite observations measure the actual total sensible heat flux H , which consists of H_a and H_n :

$$H = H_n + H_a \quad (2)$$

From the equations (1) and (2), we can calculate H_a :

$$H_a = H - R_n + G_n + LE_n \quad (3)$$

H can be obtained from the surface temperature observed by ASTER and ETM+, and the atmospheric temperature measured at ground meteorological stations using the bulk resistance approach. R_n can be estimated from the solar irradiance and atmospheric temperature monitored at meteorological stations, and from albedo and surface temperature derived from ASTER and ETM+ data. G_n was inferred from the net radiation and surface types, which were classified based on multi-spectral satellite data. LE_n is assumed to be zero in urban and suburban areas. More details are described in Kato and Yamaguchi (submitted).

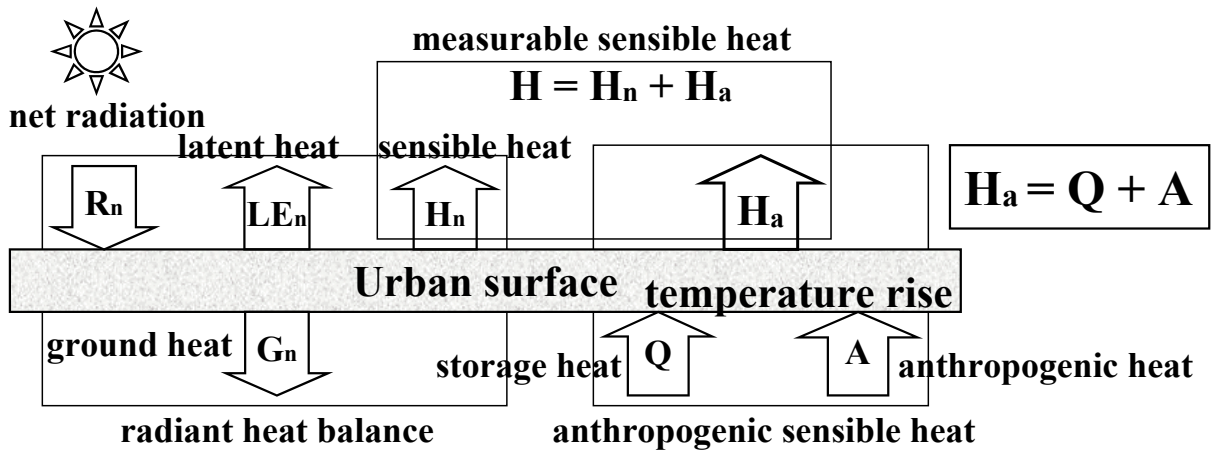


Figure 1. Concept of the urban surface heat balance.

2.2 MODIS data analysis

As the Terra and Landsat, on which ASTER and ETM+ are carried, are sun-synchronous polar orbiting satellites, data acquisition is always at the fixed local time (around 10:30 and 22:30). Moreover, as ASTER and ETM+ are high resolution sensors with relatively narrow imaging swath (60 and 180 km respectively), the recurrent period of image acquisition is 16 days. By these reasons, it is difficult to analyze temporal variations by using ASTER and ETM+. Therefore, in addition to ASTER and ETM+, we used MODIS data to know temporal variations of surface heat fluxes in urban areas. MODIS has 36 spectral bands in the visible to thermal infrared regions with 250 m to 1 km spatial resolutions and 2,330 km imaging swath. MODIS sensors are on both Terra and Aqua satellites, so that we can obtain MODIS data four times a day for the same area; at around 1:30, 10:30, 13:30, and 22:30.

The same energy balance concept in the ASTER data analysis was used for the MODIS data analysis. Net radiation R_n was estimated from the solar irradiance, surface albedo, surface temperature and emissivity, atmospheric temperature, and so on. Ground heat flux G_n was inferred from net radiation and surface types. Actual total sensible heat flux H was obtained from the surface and atmospheric temperatures. Finally, latent heat LE was calculated as the remainder of the heat balance equation. MODIS data products used were land surface temperature (LST) and emissivity; i.e., MOD11A2 (Terra/MODIS) and MYD11A2 (Aqua/MODIS) of August 21-28, 2003 (an average of 8 days), and albedo: MOD43B3 (Terra/MODIS) of August 13-28, 2003 (an average of 16 days).

3 RESULTS

The heat balance model explained in the previous chapter was applied for the ASTER and ETM+ data of spring, summer, and winter at daytime in the City of Nagoya and the surrounding areas in Japan. The increased sensible heat flux was about 100 Wm^{-2} , making up approximately 25% of the entire sensible heat in the central part of the city on July 10, 2000 (Figure 2). This is approximately twice that in the surrounding residential areas during the summer. In winter, anthropogenic heat accounted for almost all of the sensible heat flux in urban areas and reached approximately 50 Wm^{-2} in the central part of Nagoya (Figure 3). The contribution of anthropogenic heat to sensible heat flux in spring was lower than the contribution in summer and winter. The anthropogenic heat flux was high in industrial areas throughout the year. These results are consistent with the fact that anthropogenic energy consumption is high in summer and winter and low in spring.

Figure 4 shows the actual total sensible heat flux H derived from the MODIS data. In daytime, H was relatively high in the urban areas (200 to 400 Wm^{-2}) due to a large temperature difference between the land surface and atmosphere, while it was nearly zero in the other areas. In nighttime, H was nearly zero in all areas, because the land surface temperature was slightly lower than the air temperature. The diurnal variations of heat fluxes in the urban areas were shown in Figure 5. A comparison between the fluxes obtained from the ASATER and MODIS data was also shown in Figure 5. The net radiation R_n and ground heat flux G derived from the data of these two sensors coincided well. However, the absolute values of the sensible heat flux H was significantly different, although the general tendency that the urban areas show higher than the forest areas was the same. The diurnal patterns were consistent with the reported actual measurements of heat fluxes in urban areas.

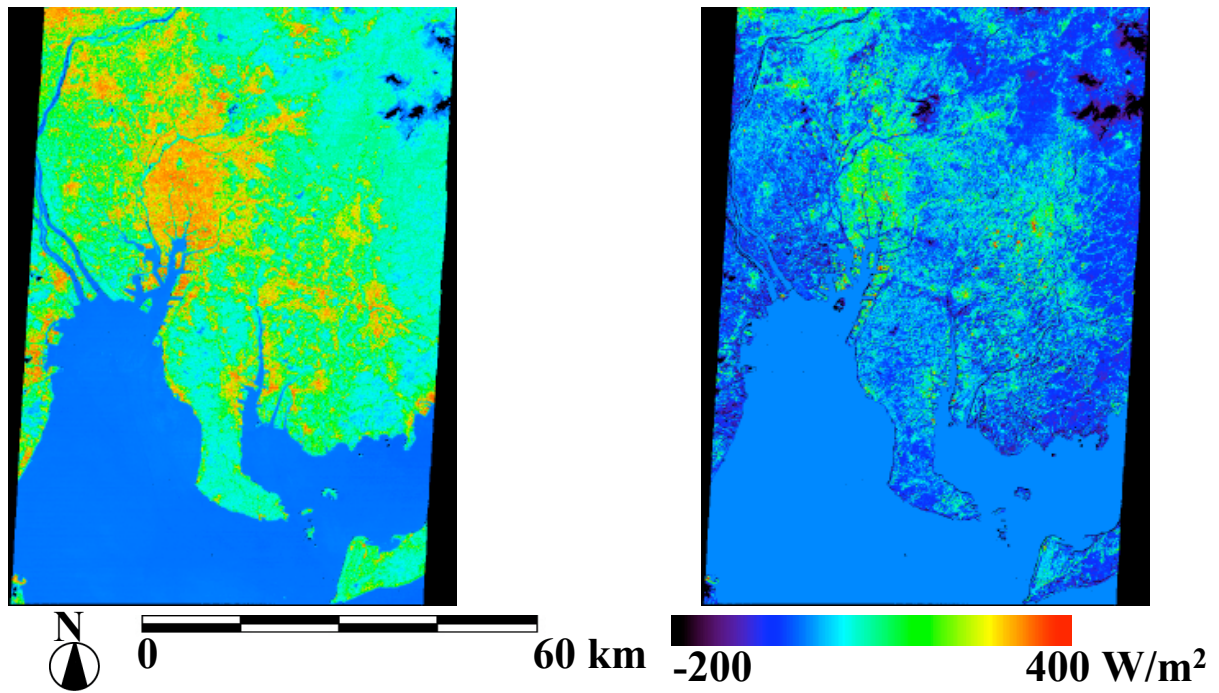


Figure 2. Natural sensible heat flux H_n (left) and anthropogenic sensible heat flux H_a (right) on July 10, 2000, in the City of Nagoya and surrounding areas.

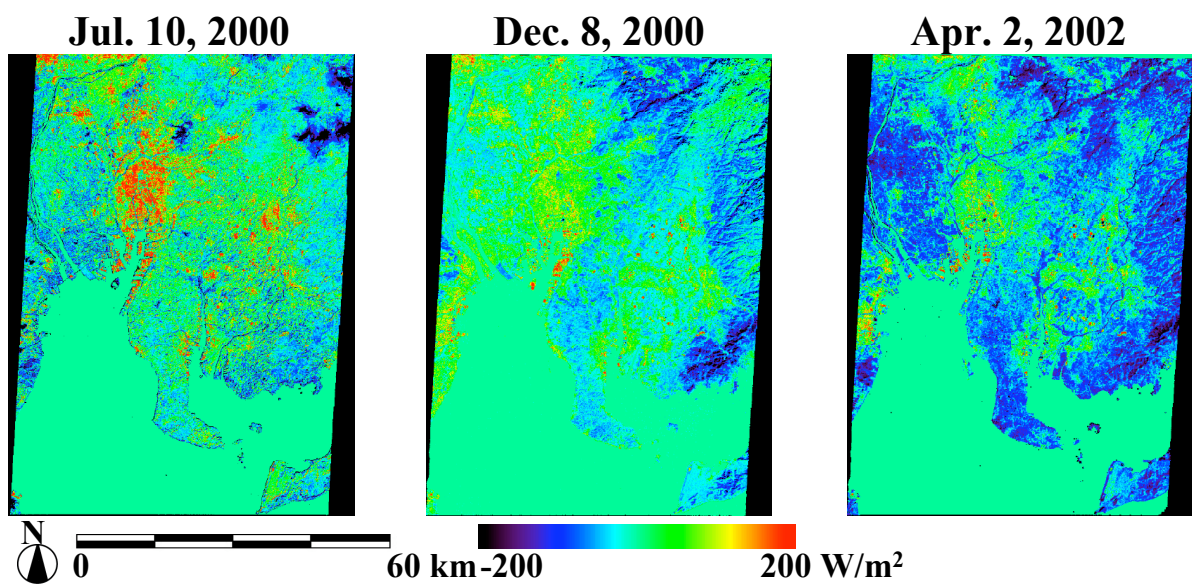


Figure 3. Anthropogenic sensible heat flux H_a on July 10, December 8, and April 2 in the City of Nagoya and surrounding areas.

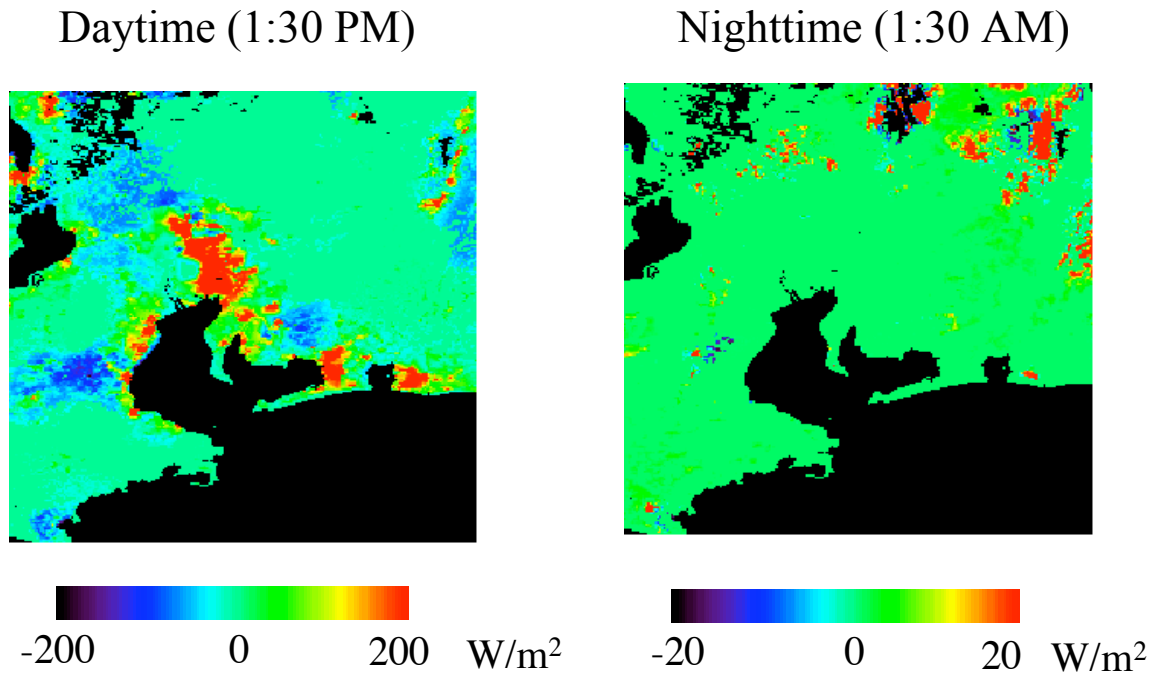


Figure 4. Sensible heat flux H in the City of Nagoya and surrounding areas, derived from the MODIS data products of August 21-28, 2003.

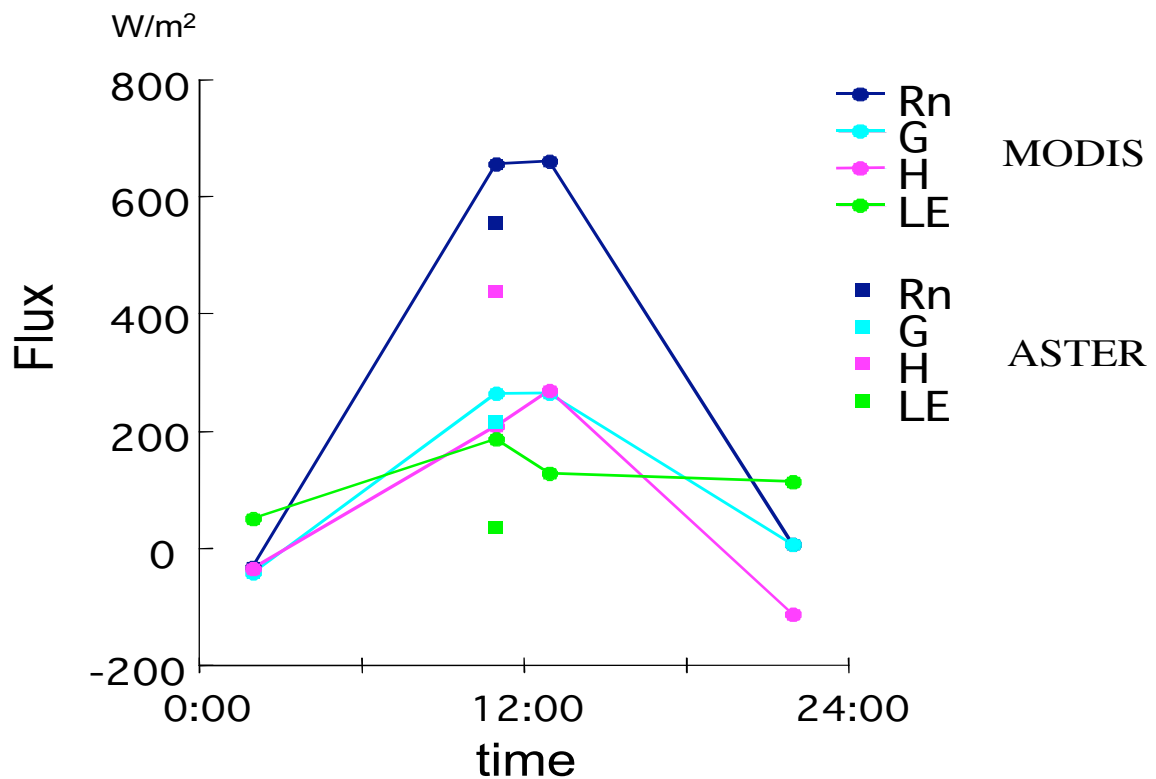


Figure 5. Temporal variation of the estimated heat fluxes in the City of Nagoya and surrounding areas, derived from the MODIS data products of August 21-28, 2003.

4 CONCLUSION

We have successfully developed a new method by which to evaluate separately the contributions of anthropogenically discharged heat and natural heat radiation to heat flux based on a heat balance model using satellite remote sensing and ground meteorological data. This method was applied for the ASTER and ETM+ data of Nagoya, Japan. Sensible heat flux due to anthropogenic activities, H_a , is useful as an index for assessing the urban heat island effect.

The spatial distribution and seasonal trends of H_a in the daytime corresponded reasonably with the actual energy consumption and solar radiation intensity. Namely, H_a was high in urban areas and low in rural areas. H_a in the central part of Nagoya was highest in July, followed by that in December, and was lowest in April. The industrial areas, in which huge amounts of energy are consumed, had extremely high H_a in all seasons. In the urban area, in July, H_a was much lower than H_n . Therefore, the decrease in vegetation is thought to be the most significant contributor to the heat island effect on summer days.

We analyzed the MODIS data in summer. There were significantly large temporal variations in net radiation. In daytime, the sensible heat flux was high in urban areas, while it was nearly zero in all areas in nighttime. This study showed that combination of ASTER/ETM+ and MODIS data is a powerful tool to analyze the spatial and temporal variations of surface heat fluxes in urban areas.

5 ACKNOWLEDGEMENTS

The authors wish to thank the ASTER Science Team members for their helpful discussions. The ASTER data were provided by the Earth Remote Sensing Data Analysis Center (ERSDAC). This research was partially supported by grants from the Ministry of Education, Culture, Sports, Science and Technology, Japan (Dynamics of the Sun-Earth-Life Interactive System, No.G-4, the 21st Century COE Program, and Grant-in-Aid for Scientific Research, No.14580101, 2002-2004).

6 REFERENCES

- Kato, S., and Yamaguchi, Y., Analysis of urban heat island effect using ASTER and ETM+ data –separation of anthropogenic heat discharge and natural heat radiation in sensible heat flux. *Remote Sensing of Environment*, submitted.
- Schmugge, T.J., Kustas, W.P., and Humes, K.S., 1998, Monitoring land surface fluxes using ASTER observations. *IEEE Transactions on Geoscience and Remote Sensing*, 36, 1421-1430.
- Yamaguchi, Y., Kahle, A.B., Tsu, H., Kawakami, T., and Pniel, M., 1998, Overview of Advanced Spaceborne Thermal Emission and Reflection Radiometer (ASTER). *IEEE Transactions on Geoscience and Remote Sensing*, 36, 1062-1071.
- Yamaguchi, Y., Fujisada, H., Tsu, H., Sato, I., Watanabe, H., Kato, M., Kudoh, M., Kahle, A.B., and Pniel, M., 2001, ASTER early image evaluation. *Advances in Space Research*, 28 (1), 69-76.